Int. J. Electrochem. Sci., 9 **(2014)** 8145 - 8154

International Journal of
ELECTROCHEMICAL
SCIENCE
www.electrochemsci.org

Preparation and Characterization of Electrodeposited Ni-CeO_2 Nanocomposite Coatings with High Current Density

Y.B. Zeng[1, 2], *N.S. Qu*[1, 2, *] *and X.Y. Hu*[1]

[1]College of Mechanical and Electrical Engineering, Nanjing University of Aeronautics and Astronautics, Nanjing 210016, P.R. China
[2]Jiangsu Key Laboratory of Precision and Micro-Manufacturing Technology, Nanjing 210016, P.R. China
[*]E-mail: nsqu@nuaa.edu.cn

Received: 13 August 2014 / *Accepted:* 14 October 2014 / *Published:* 28 October 2014

Nanocomposite coatings have been widely used in various engineering applications. At present, direct current electrodeposition is still a widely used method for preparing nanocomposite coatings. However, in previous studies, the maximum current density for preparing Ni-CeO_2 nanocomposite coatings was only 5.4 A dm^{-2} because of the limiting current density. In this study, a high current density of 8 A dm^{-2} was used to prepare Ni-CeO_2 nanocomposite coatings by direct current electrodeposition. Flushing with a strong electrolyte thinned the diffusion layer and increased the limiting current density. The properties of the electrodeposited Ni-CeO_2 nanocomposite coatings were characterized. Increasing the bath concentration of the CeO_2 nanoparticles increased the weight percent of CeO_2 particles in the nanocomposite coatings, and improved the microhardness, and the friction, corrosion, and wear behavior of the coatings. However, excessive CeO_2 nanoparticle loadings were detrimental to the coating properties. Furthermore, incorporating CeO_2 particles into the coatings altered the morphology and preferred orientation of the composite coatings.

Keywords: Ni-CeO_2 nanocomposite coatings; High current density; Electrodeposition; Corrosion behavior

1. INTRODUCTION

Nanocomposite coatings have been widely used in various engineering applications [1-3]. The fabrication and characterization of nanocomposite coatings prepared by electrodeposition has been extensively investigated. Many types of nanoparticles, including SiC, Al_2O_3, ZrO_2, PSZ, carbon nanotubes, and diamond, have been used in electrodeposited nanocomposite coatings [4-10].

Cerium oxide (CeO_2), a rare earth oxide, has attracted considerable interest in metal-matrix composite coatings. Balathandan et al. reported that a Ni matrix reinforced with micron-sized CeO_2 particles displayed good corrosion resistance compared with that of Ni-ZrO_2, Ni-PSZ, and pure Ni coatings [11]. Li et al. prepared Ni–Zn/CeO_2 composite electrodes and investigated the effects of CeO_2 on the hydrogen evolution reaction activity [12]. Shahrabi et al. illustrated a new procedure for electrodeposition of Ni-cerium oxide amorphous-nano crystalline composite coatings, in which the metal and oxides are deposited simultaneously on the samples from the plating bath solution containing Ni ions and Ce ions with no powder added [13].In composite electrodeposition, current density plays a key role in the microstructure and properties of composite coatings. Aruna et al. investigated the properties of electrodeposited Ni-CeO_2 nanocomposite coatings, which were prepared at current densities of 0.23, 0.77, 1.55, 3.1, and 5.4 A dm^{-2}, and demonstrated that the properties are closely related to the applied current density [14]. Subramania et al. prepared Cu-CeO_2 composite coatings by electrodeposition at a current density of 5 A dm^{-2} [15]. Xue et al. electrodeposited Ni–CeO_2 composite coatings at a current density of 4 A dm^{-2}, and found that that the electrodeposition method can significantly affect the microstructure and oxidation resistance of Ni–CeO_2 nanocomposite coatings and those of pure Ni coatings [16]. Srivastava et al. reported the structure and properties of NiCo-CeO_2 nanocomposite coatings obtained at a current density of 0.8 A dm^{-2} [17]. Venkatesha et al. observed the crystal structure, texture, surface morphology, and electrochemical corrosion behavior of Zn-CeO_2 nanocomposite coatings synthesized at a constant current density of 4 A dm^{-2} [18]. Co-CeO_2 nanocomposite coatings electrodeposited at a constant current density of 2.3 A dm^{-2} exhibited higher polarization resistance compared with Co layers in simulated body fluid [19].

At present, direct current electrodeposition is still a major method for preparing composite coatings. In direct current electrodeposition, the maximum applied current density in previous reports is about 5.4 A dm^{-2} because of the limiting current density. The applied current density has a large effect on the composition, morphology, preferred orientation, and properties of the deposits containing CeO_2 particles. The maximum applied current density may be substantially increased by using a pulsed current. Das et al. investigated the effect of the pulse peak current on the crystallite size and microhardness of the Ni-CeO_2 coatings obtained by pulse electrodeposition, and found that the microhardness increased with the current density. However, the coelectrodeposited CeO_2 content in the nickel matrix increased up to a current density of 50 A dm^{-2}, beyond which it decreased [20]. In our previous studies, composite coatings were prepared by flushing with a strong electrolyte [21], which allowed a high current density to be applied, probably because the process thinned the diffusion layer and increased the limiting current density. However, the fabrication of Ni-CeO_2 nanocomposite coatings by direct current electrodeposition with a high current density has still not been investigated thoroughly. This paper reports the composition, morphology, preferred orientation, microhardness, wear resistance, and corrosion resistance of Ni-CeO_2 nanocomposite coatings obtained by direct current electrodeposition with a high current density.

2. EXPERIMENTAL

The gap between the cathode and anode positioned in parallel was about 2 mm (Fig. 1). An insoluble platinum plate, 70 × 60 × 3 mm, was used as the anode, and the stainless steel specimen, 70 × 60 × 1 mm, was used as the cathode. Table 1 shows the electrolyte used in the present study. Before the composite electrodeposition, the electrolyte was pumped from the tank into the inter-electrode gap for 120 min to disperse the nanosized particles.

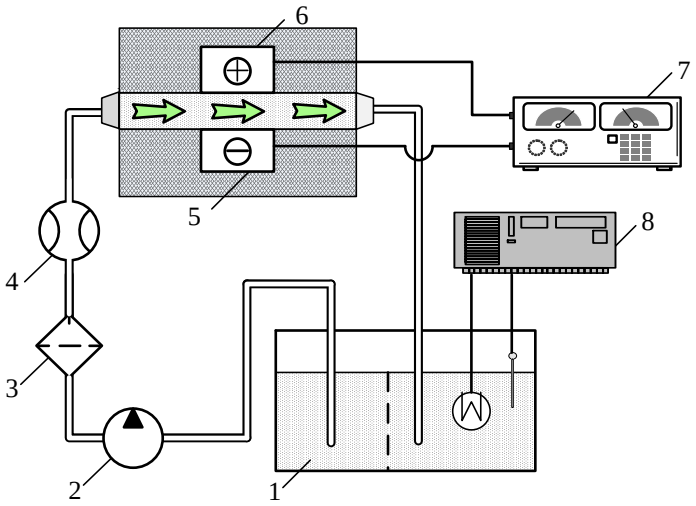

1. Electrolyte cell, 2. Electrolyte supply pump, 3. Filter , 4. Flow meter,
5. Cathode, 6. Anode, 7.Power generator, 8. Temperature control unit

Figure 1. Schematic of the co-deposition apparatus.

Table 1. Composition of the electrodeposition bath.

Component	Amount
Nickel sulfamate	350 g L^{-1}
Ammonium chloride	15 g L^{-1}
Sodium dodecyl sulphate	0.1 g L^{-1}
Boric acid	35 g L^{-1}
CeO_2 nanoparticles with a diameter of 20–30 nm	10, 20, 30, 40 g L^{-1}
Bath temperature	50 ± 1 °C

The deposition thickness for each sample was fixed as 50 μm by altering the deposition time. The surface morphology of the deposits was examined by scanning electron microscope (SEM; S3400N, Hitachi, Japan), and the composition of the deposits was determined by the energy dispersive spectrum (X-Flash 5010, Bruker, Germany) attached to the SEM. The microhardness of the deposits was measured by a micro-hardness tester (HXS-1000A, Shanghai Shangguang Instrument Plant, China) under a load of 100 g for 15 s. The wear resistance of the deposits was measured with an applied load of 4.98 N, a frequency of 2.5 Hz, and a time of 10 min. An electrochemical work station (CHI660d, Shanghai Chenhua, China) was used to test the electrochemical corrosion behavior of the

Ni and Ni–CeO_2 nanocomposite coatings in 3.5% NaCl solution, in which a Pt plate and a saturated calomel electrode (SCE) were used as the counter electrode and the reference electrode, respectively.

3. RESULTS AND DISCUSSION

3.1 Composition, morphology, and preferred orientation of coatings

Figure 2 shows the change in the weight percent of CeO_2 nanoparticles incorporated into the Ni-CeO_2 nanocomposite coatings as the CeO_2 nanoparticle bath concentration increased from 0 to 40 g L^{-1} at a current density of 8 A dm^{-2}. The weight percent of coelectrodeposited CeO_2 nanoparticles in the coatings was 1 wt % for a CeO_2 nanoparticle bath concentration of 10 g L^{-1}, and this increased significantly with the increase in the bath concentration. The maximum weight percent of coelectrodeposited particles in the coatings, 3.13 wt %, is observed at a CeO_2 nanoparticle bath concentration of 30 g L^{-1}. However, the CeO_2 nanoparticles embedded in the deposits was reduced to 0.74 wt % when the CeO_2 nanoparticle bath concentration was further increased to 40 g L^{-1}.

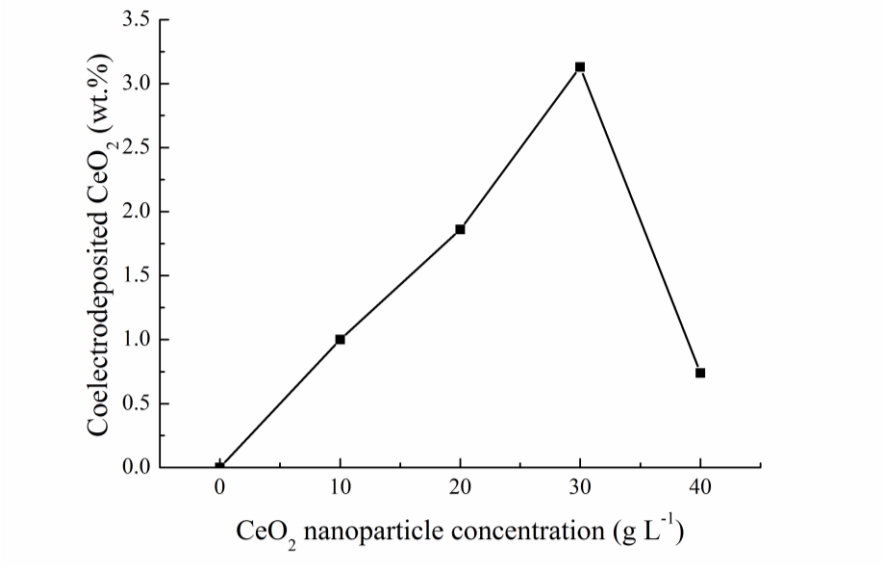

Figure 2. Weight percent of CeO_2 nanoparticles in the Ni-CeO_2 composite coatings prepared at different CeO_2 nanoparticle bath concentrations.

The morphologies of the Ni and Ni-CeO_2 coatings prepared at different CeO_2 nanoparticle bath concentrations at a current density of 8 A dm^{-2} are shown in Fig. 3. The morphology of the coatings changed with the incorporation of CeO_2 nanoparticles in the deposits. Notably, the pits in the morphology shown in Fig. 3e were observed at a CeO_2 nanoparticle bath concentration of 40 g L^{-1}. The agglomeration of CeO_2 nanoparticles would occur when the bath concentration of CeO_2 nanoparticles was too high. Some of the CeO_2 nanoparticles adsorbed on the surface of the deposits were removed because of the effect of the agglomerates on these adsorbed CeO_2 nanoparticles at a high electrolyte flow rate, which produces the pits.

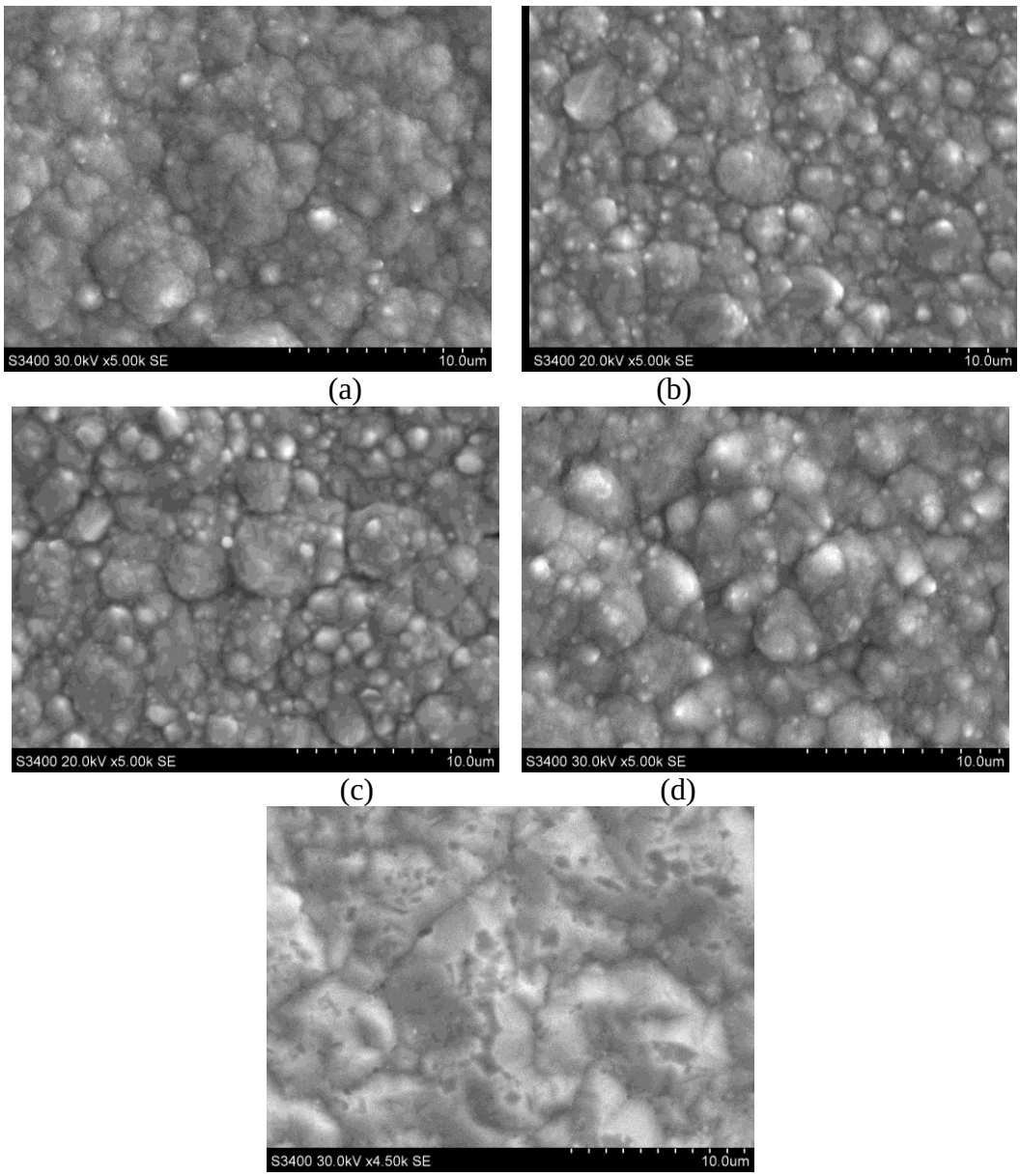

Figure 3. Morphology of Ni-CeO_2 nanocomposite coatings at a current density of 8 A dm^{-2} and CeO_2 particle bath concentrations of (a) 0, (b) 10, (c) 20, (d) 30, and (e) 40 g L^{-1}.

The preferred orientation of Ni and Ni-CeO_2 coatings was also investigated by using XRD. Figure 4a shows that for pure nickel, the (200) orientation was the most intense peak, which is probably because the bath was free of inhibiting chemical species. When CeO_2 nanoparticles were added to the bath, the CeO_2 nanoparticles embedded in the deposits played a major role in nickel crystal growth, which reduced the relative intensity of the (200) orientation and increased that of the (111), (220), and (311) orientations considerably (Fig. 4b–e). Moreover, the relative intensity of the (111) orientation is greatest when the coelectrodeposited CeO_2 nanoparticles content is highest, which is obtained at the CeO_2 nanoparticle bath concentration of 30 g L^{-1}.

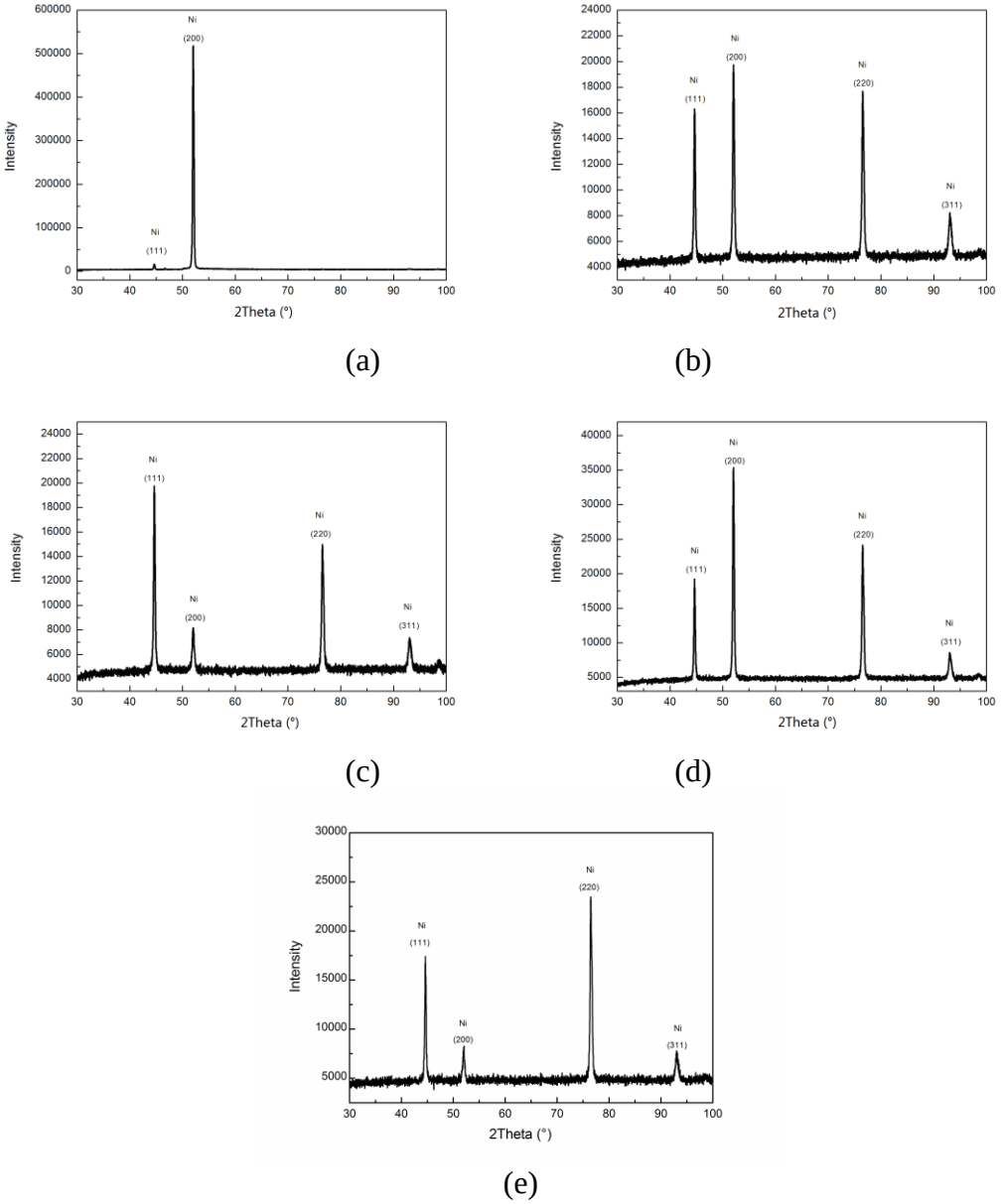

Figure 4. XRD patterns of Ni–CeO_2 nanocomposite coatings obtained at a current density of 8 A dm^{-2} with CeO_2 particle bath concentrations of (a) 0, (b) 10, (c) 20, (d) 30, and (e) 40 g L^{-1}.

3.2 Microhardness and wear resistance of coatings

The microhardness of the Ni and Ni-CeO_2 coatings obtained at a current density of 8 A dm^{-2} with various CeO_2 particle bath concentrations were measured. Figure 5 shows that the microhardness of the deposits increased with the addition of CeO_2 nanoparticles to the bath. The maximum microhardness of deposits, 436 Hv, was obtained at a CeO_2 nanoparticle bath concentration of 30 g L^{-1}. When the CeO_2 nanoparticle bath concentration was increased to 40 g L^{-1}, the microhardness was reduced to 279 Hv, which is lower than that of Ni coatings. Because the CeO_2 nanoparticles incorporated into the coatings hinder the movement of dislocations, the microhardness of the deposit

with a large amount of CeO_2 nanoparticles incorporated was increased. The microhardness was reduced when pits in the deposit formed.

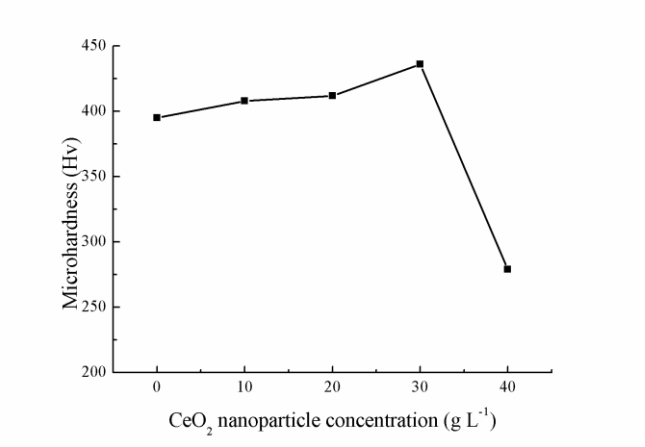

Figure 5. Microhardness of Ni–CeO_2 nanocomposite coatings obtained at a current density of 8 A dm^{-2} at various CeO_2 particle bath concentrations.

Figure 6 shows the friction coefficient and wear weight loss of the Ni and Ni-CeO_2 coatings obtained at a current density of 8 A dm^{-2} with various CeO_2 particle bath concentrations. For pure nickel, the friction coefficient was 0.283, and the wear weight loss was 4.9 mg. Adding CeO_2 particles decreased the friction coefficient and wear weight loss of the Ni-CeO_2 coatings. The minimum values of the friction coefficient and wear weight loss were 0.157 and 3.2 mg, respectively, and these were obtained at a CeO_2 nanoparticle bath concentration of 30 g L^{-1}. When the CeO_2 nanoparticle bath concentration was increased to 40 g L^{-1}, the values rose to 0.357 and 5.2 mg, respectively, which are larger than those of the Ni coating. These trends are similar to those observed for the microhardness of nanocomposite or microcomposite coatings, as reported by Zhang et al. [22], Zhou et al. [23] and Ibrahim et al. [24].

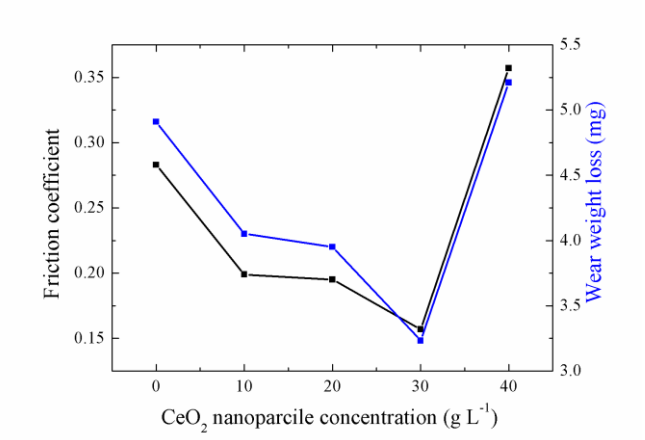

Figure 6. Wear resistance of Ni–CeO_2 nanocomposite coatings obtained at a current density of 8 A dm^{-2} with various CeO_2 particle bath concentrations.

3.3 Electrochemical characterization of coatings

Figure 7 shows the potentiodynamic polarization curves of Ni and Ni-CeO_2 coatings obtained at a current density of 8 A dm^{-2} with various CeO_2 particle bath concentrations. Different parameters, such as the corrosion potential, E_{corr}, the corrosion current density, i_{corr}, and the anodic/cathodic Tafel slopes (βa and βc) derived from Fig. 7, are summarized in Table 2. The E_{corr} and i_{corr} values of pure nickel coating are 891 mV and 36.7 A cm^{-2}, respectively, and they were decreased by the addition of CeO_2 particles to the bath. The minimum values of E_{corr} and i_{corr} were 444 mV and 2.97 A cm^{-2}, and were observed for a CeO_2 nanoparticle bath concentration of 30 g L^{-1}. When the CeO_2 nanoparticle bath concentration increased to 40 g L^{-1}, they rose to 813 mV and 30.2 A cm^{-2}. Comparing to the other samples, the sample (C_{CeO2}=30 g L^{-1}) has the highest values of anodic and cathode slopes (9.834 and 13.574, respectively), seeing Table 2. This may be explained by the fact that anodic and cathodic reactions are difficult to occur owing to the uniform and compact coatings. Therefore, the Ni-CeO_2 coating with the highest weight percent of CeO_2 (3.13 wt %) had the lowest rate of corrosion. It can be concluded that the presence of CeO_2 particles in coatings improved the corrosion behavior of coatings significantly. Venkatesha et al. [18] , Benea [19] and Muresan et al. [25] also observed that the incorporation of particles significantly affected the corrosion behavior of composite coatings.

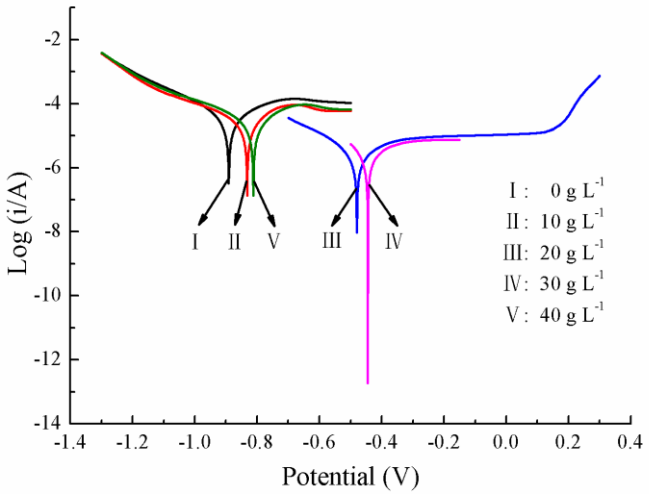

Figure 7. Tafel curves of Ni and the Ni-CeO_2 nanocomposite coatings in 3.5% NaCl solution while CeO_2 particle bath concentrations of (Ⅰ) 0, (Ⅱ) 10, (Ⅲ) 20, (Ⅳ) 30, and (Ⅴ) 40 g L^{-1}.

Table 2. Corrosion potential and current density of Ni and Ni-CeO_2 coatings.

CeO_2 nanoparticle bath concentration/ g L^{-1}	E_{corr}/mV	i_{corr}/A cm^{-2}	βa (1/V)	βc (1/V)
0	891	36.7	4.742	5.918
10	833	31.4	4.613	4.751
20	483	3.07	3.983	6.181
30	444	2.97	9.834	13.754
40	813	30.2	4.742	4.950

4. CONCLUSIONS

In this work, a high current density of 8 A dm^{-2} was used to prepare Ni-CeO_2 nanocomposite coatings during direct current electrodeposition. Flushing with a strong electrolyte thinned the diffusion layer and increased the limiting current density. According to the experimental results, the following conclusions can be drawn.

(1) The weight percent of CeO_2 particles in the nanocomposite coatings increased with the loading of CeO_2 nanoparticles from 10 to 30 g L^{-1} at a current density of 8 A dm^{-2}. Increasing the CeO_2 nanoparticle concentration to 40 g L^{-1} reduced the weight percent of CeO_2 particles in the nanocomposite coatings.

(2) The incorporation of CeO_2 nanoparticles altered the morphology and preferred orientation of the composite coatings.

(3) The microhardness, friction, and wear behavior of the coatings were improved as the amount of CeO_2 nanoparticles incorporated into the metal matrix increased up to a CeO_2 nanoparticle bath concentration of 30 g L^{-1}. Increasing the bath concentration further reduced the microhardness of composite coatings to less than that of pure nickel, and increased the friction coefficient and wear weight loss to greater than those of pure nickel.

(4) The incorporation of CeO_2 particles into coatings improved the corrosion behavior of the coatings significantly.

ACKNOWLEDGEMENTS

The work in this study was supported by the Joint Funds of the National Natural Science Foundation of China and Guangdong Province (grant no. U1134003) and the Jiang Su Natural Science Foundation (grant no. BK20131361).

References

1. S.O. Yilmaz, M. Özenbas and M. Yaz, *Mater. Manuf. Process.* 26 (2011) 722–731
2. J. Hu, L. Fang and P.W. Zhong, *Mater. Manuf. Process.* 28 (2013) 1294–1300
3. E. Aghaie, A. Najafi, H. Maleki-Ghaleh and H. Mohebi, *Surf. Eng.* 29 (2013) 177–182
4. M. Mulukutla, A. Singh and S.P. Harimkar, *T. I. Met. Finish.* 90 (2012) 316–323
5. A. Shamsolhodaei, H. Rahmani and S. Rastegari, *Surf. Eng.* 29 (2013) 695–699
6. F. C. Walsh and C. Poncen de Leon, *T. I. Met. Finish* 92 (2014) 83–98
7. W. Huang, Y.W. Zhao and X.L. Wang, *Surf. Coat. Tech.* 235 (2013) 489–494
8. Y. Yang and Y.F. Cheng, *Electrochim. Acta.* 109 (2013) 638–644
9. K.A. Kumar, P. Mohan, G.P. Kalaignan and V.S. Muralidharan, *J. Nanosci. Nanotechno.* 12 (2012) 8364–8371
10. S.T. Aruna and K.S. Rajam, *Scripta Mater.* 48 (2003) 507–512
11. S. Balathandan and S.K. Seshadri, *Met. Finish.* 92 (1994) 49–53
12. Z. Zheng, N. Li, C.Q. Wang, D.Y. Li, F.Y. Meng and Y.M. Zhu, *J. Power Sources* 222 (2013) 88–91
13. H. Hasannejad, T. Shahrabi, M. Jafarian and A. Sabour Rouhaghdam. *J. Alloy. Compd.* 509 (2011) 1924–1930
14. S.T. Aruna, C.N. Bindu, V. Ezhil Selvi, V.K. William Grips and K.S. Rajam, *Surf. Coat. Tech.*

200 (2006) 6871–6880
15. S. Ramalingam, V.S. Muralidharan and A. Subramania, *Surf. Eng.* 29 (2013) 511–515
16. Y.J. Xue, H.B. Liu, M.M. Lan, J.S. Li and H. Li, *Surf. Coat. Tech.* 204 (2010), 3539–3545
17. M. Srivastava, V.K.W. Grips and K.S. Rajam, *Appl. Surf. Sci.* 257 (2010) 717–722
18. S. Ranganatha, T.V. Venkatesha, K. Vathsala and M.K. Punith kumar, *Surf. Coat. Tech.* 208 (2012) 64–72
19. L. Benea, *Metall. Mater. Trans. A* 44 (2013) 1114–1122
20. R.J. Sen, S. Das and K. Das, *J. Nanosci. Nanotechno.* 10 (2010) 8217–8226
21. N.S. Qu, W.H. Qian, X.Y. Hu and Z.W. Zhu, *Mater. Manuf. Process.* 29 (2014) 37–41
22. Z. Zhang, X. Wu, C. Jiang and N. Ma, *Surf. Eng.* 30 (2014) 21–25
23. X.W. Zhou and Y.F. Shen, *Surf. Coat. Tech.* 249 (2014) 6–18
24. M.A.M. Ibrahim, F.Kooli and S.N. Alamri, *Int. J. Electrochem. Sci.* 8(2013), 12308-12320
25. P.L. Nemes, M.lekka, L. Fedrizzi, and L.M. Muresan, *Surf. Coat. Tech.* 252 (2014), 102–107